Acta Biochim Biophys Sin xxxx, xx(x): xx-xx
https://cstr.cn/32197.14.abbs.2026115
https://doi.org/10.3724/abbs.2026115
Original Article

Original Article

Signal peptide-mediated endoplasmic reticulum targeting enhances antigen expression and secretion to improve mRNA vaccine efficacy

Zijia Guo[1,2,†], Luna Ran[1,2,†], Jiayan Fu[1,2], Nengcheng Bao[1,2], Han Hu[1,2], Zimo Wu[3], Haiyang Dong[2], Yuanhui Mao[4], and Yongfeng Jin[1,2,3,*]

[1]National Key Laboratory of Advanced Drug Delivery and Release Systems, Zhejiang University, Hangzhou 310058, China, [2]MOE Laboratory of Biosystems Homeostasis & Protection, Innovation Center for Cell Signaling Network, College of Life Sciences, Zhejiang University, Hangzhou 310058, China, [3]School of Life Science, Zhejiang Chinese Medical University, Hangzhou 310058, China, and [4]Department of Urology of The Second Affiliated Hospital & Liangzhu Laboratory, Zhejiang University School of Medicine, Zhejiang University, Hangzhou 310058, China
[†]These authors contributed equally to this work.
*Correspondence address. E-mail: jinyf@zju.edu.cn

Received 11 February 2026 Accepted 10 June 2026 Published 3 August 2026

Abstract
The expression and secretion levels of antigenic proteins are critical determinants of mRNA vaccine efficacy. Signal peptides, which direct protein translocation into the endoplasmic reticulum (ER), have the potential to significantly enhance protein expression and immunogenicity, highlighting their value as engineering tools for mRNA vaccine design. This study adopts the SARS-CoV-2 RBD as a model antigen to screen a panel of signal peptides derived from common secretory proteins. The signal peptides from C3, IL-12, and IL-20 are identified as candidates capable of significantly promoting antigen expression and secretion. Fluorescence confocal microscopy reveals that these signal peptides enhance the targeting of mRNA to the ER at the subcellular level. *In vivo* experiments demonstrate that mRNA vaccines incorporating these engineered signal peptides induce stronger humoral and cellular immune responses. This study confirms that signal peptide replacement can enhance antigen expression, offering a potential strategy for improving the efficacy of mRNA vaccines.

Key words signal peptide, endoplasmic reticulum localization, mRNA targeting, mRNA vaccine, efficacy

Introduction

In recent years, messenger RNA (mRNA) vaccine technology has advanced rapidly, with several candidate vaccines targeting infectious diseases having been approved or entering clinical trials [1]. Most mRNA vaccines are delivered via lipid nanoparticles (LNPs) into muscle or intradermal tissues, where they are translated into antigenic proteins to elicit adaptive immunity [2,3]. Although mRNA vaccines offer advantages such as rapid development, reduced costs, scalable manufacturing, and strong immunogenicity, their broader application still faces numerous challenges, including the need to further improve delivery efficiency, *in vivo* stability, and translational output. Therefore, optimizing mRNA sequence design, delivery systems, and translation regulation to enhance antigen yield and immunogenicity remains an area requiring further exploration [4–11].

Previous studies have shown that replacing signal peptides can enhance the expression and secretion of downstream proteins in mammalian cells [12,13]. Signal peptides mediate co-translational endoplasmic reticulum (ER) targeting via the signal recognition particle (SRP), positioning translating mRNAs within a ribosome-rich and secretion-competent environment [14,15]. Additionally, as a central hub of the secretory pathway and protein folding machinery, the ER facilitates the efficient processing and secretion of nascent polypeptides [15–17]. Taken together, these features suggest that signal peptide-mediated ER targeting may concurrently enhance both translational output and secretory capacity [18,19]. Therefore, it is hypothesized that engineering signal peptides could enhance mRNA-ER co-localization, thereby synergistically improving both translational output and secretory capacity, ultimately boosting the efficacy of mRNA vaccines.

© The Author(s) 2026. This is an open access article distributed under the terms of the Creative Commons Attribution License (https://creativecommons.org/licenses/by/4.0/).

This study used the SARS-CoV-2 RBD as a model antigen to screen a panel of natural human signal peptides, identifying C3, IL-12 and IL-20 as candidates capable of markedly enhancing antigen expression and secretion. Confocal imaging demonstrated that these signal peptides promote mRNA targeting to the ER at the subcellular level, providing mechanistic support for their translational advantage. *In vivo* analyses further demonstrated that incorporating these engineered signal peptides into mRNA vaccines elicits stronger humoral and cellular immune responses. Taken together, these findings establish signal peptide engineering as a rational and broadly applicable strategy for enhancing the efficacy of mRNA vaccines.

Materials and Methods

Cell lines and animals

293T and HeLa cells were purchased from Hai Xing Biosciences (Suzhou, China); RAW264.7 cells were purchased from Zhejiang Noble Biological Products Co., Ltd (Hangzhou, China); and DC2.4 cells were purchased from Shanghai Biowing Applied Biotechnology (Shanghai, China). Culture conditions consisted of DMEM (Gibco, Grand Island, USA) supplemented with 10% fetal bovine serum (FBS; Gibco) and 1% penicillin/streptomycin (Gibco) for 293T, HeLa, and RAW264.7 cells, whereas DC2.4 cells were maintained in RPMI 1640 medium (Gibco) containing the same concentrations of FBS and antibiotics.

Female BALB/c mice (6 weeks old) were obtained from Qi Zhen Laboratory Animal Tech Co. Ltd. (Hangzhou, China), and used for vaccination. The animals were housed under controlled environmental conditions (22 ± 2.0°C, 50% ± 10% humidity) with a 12/12 h light/dark cycle and provided a standard diet and tap water. All procedures were conducted in compliance with the China Public Health Service Guide for the Care and Use of Laboratory Animals and were approved by the Animal Ethical Committee of Zhejiang University and the Use Committee of Zhejiang University (No. ZJU20260480).

Synthesis of mRNA

Coding sequences for the receptor-binding domain (RBD) of SARS-CoV-2 surface glycoprotein (YP_009724390), the fusion protein of respiratory syncytial virus (NP_044596.1), and Ebola glycoprotein (NP_066246.1) were individually cloned and inserted into linearized template vectors (Takara Biotech, Dalian, China) using seamless cloning to generate plasmid constructs for *in vitro* transcription (Supplementary Table S1).

mRNA was synthesized using standard *in vitro* transcription methods. Plasmids encoding specific antigens were digested for 2.5 h with *Hin*dIII to obtain a linearized template. *In vitro* transcription was performed using the T7 High Yield RNA Transcription Kit (Vazyme, Nanjing, China) with complete substitution of UTP by N^1-methyl-pseudouridine following established protocols [20]. Synthesized mRNA was subsequently purified with the EasyPure RNA Purification Kit (TransGen Biotech, Beijing, China), analyzed by agarose gel electrophoresis, and stored at −80°C.

Preparation and characterization of mRNA-LNP

Lipid nanoparticles (LNPs) were formulated according to the disclosed prescription by Moderna (Cambridge, USA) [21]. The lipid mixture comprising ionizable lipid SM102, cholesterol CHOHP, DSPC, and DMG PEG-2000 (AVT, Shanghai, China) was mixed at a mass ratio of 50:10:38.5:1.5 in absolute ethanol. Three volumes of mRNAs [1:25 (w/w) mRNA to lipid, nitrogen/phosphate (N/P) ratio of 6] were suspended in sodium citrate buffer (pH 4.5). The two solutions were rapidly mixed by pipetting. The resulting mRNA-LNPs were dialyzed in PBS for further analysis. Particle morphology was examined by transmission electron microscopy (JEM-1400 Flash; JEOL, Tokyo, Japan). Size distribution and zeta potential were measured using dynamic light scattering (Zetasizer Nano ZS90; Malvern Instruments, Malvern, UK).

Analysis of mRNA expression

For luciferase activity assays, cells were seeded in 48-well plates at 4×10^5 cells/well. At 60%–70% confluence, transfections were performed with 200 ng of target mRNA together with 200 ng of Firefly luciferase (Fluc) mRNA as an internal control. After 24 h, NanoLuc activity was quantified using the Nano-Glo® Luciferase Assay System (Promega, Madison, USA) on Multimode Plate Reader (VICTOR Nivo; Thermo Fisher Scientific, Waltham, USA).

For ELISA, cells were plated in 12-well plates at 1×10^5 cells/well and transfected with 1 μg of mRNA per well at similar confluence. Culture supernatants and cell lysates were collected 24 h post-transfection and analyzed using a SARS-CoV-2 Spike RBD ELISA Kit (SinoBiological, Beijing, China).

Endoplasmic reticulum targeting assay

Cells were plated on glass coverslips in 6-well plates at 4×10^5 cells per well. At 60%–70% confluence, the SEC61B-GFP plasmid was transfected using Lipofectamine 3000 (Thermo Fisher Scientific). After 24 h, Cy5-mRNA-LNPs were added and incubated for 4 h. Cells were then washed with DPBS, fixed with 4% paraformaldehyde, stained with DAPI, and mounted with ProLong Diamond Antifade Mountant (Invitrogen, Carlsbad, USA). The periphery of the coverslip was sealed with nail polish and finally imaged using CLSM (FLUOVIEW FV3000 CLSM; Olympus, Tokyo, Japan) [22]. For each group, 20 cells were randomly selected for quantitative analysis.

In vivo expression and bioluminescence imaging

Female BALB/c mice (6 weeks old) received an intramuscular injection of RBD mRNA-LNPs. At 6, 12, 24, and 48 h post-administration, mice were injected with 100 μL of luciferin (15 mg/mL; Guangzhou Biolight Biotechnology, Guangzhou, China). After 10 min, bioluminescence signals were captured using an IVIS Spectrum *in vivo* imaging system (Caliper Life Sciences, Hopkinton, USA).

Splenocyte restimulation with antigenic peptides

Spleens from immunized mice were aseptically processed and passed through a 45-μm cell strainer. Following red blood cell lysis, splenocytes were resuspended in RPMI 1640 medium with 10% FBS. Cells (1×10^6 per well) were seeded in 24-well plates and stimulated with 20 ng of antigenic peptide per well for 24 h at 37°C. Brefeldin A (Invitrogen) was added for the final 4 h before harvest for flow cytometric analysis.

Flow cytometry for immune cells and antibodies

Antibodies for flow cytometry analysis were purchased from

BioLegend Inc. (San Diego, USA) and listed in Supplementary Table S2. Cells were incubated with TruStain FcX™ (anti-mouse CD16/32) antibody for 20 min, followed by staining with fluorophore-conjugated antibodies on ice for 30 min. Cells were subjected to permeabilization using Permeabilization Buffer (10×) (eBioscience, San Diego, USA), diluted to 1× with distilled water, and incubated at 4°C for 30 min. Thereafter, cells were stained with anti-IFN-γ and anti-IL-4 antibodies at 4°C for 30 min in the dark. After washing, the cells were evaluated by flow cytometry (CytoFLEX, Beckman Coulter, US) and analyzed using FlowJo software. The gating strategies for T cells and B cells in this study are shown in Supplementary Figure S1.

ELISA for antibody titer

The antigen-specific antibody titer was measured using an indirect ELISA kit from Acrobiosystems (Beijing, China). The diluted serum (1:1600 dilution) was added to the plates and incubated for 1 h at 37°C. After incubation and washing, plates were treated with HRP-conjugated anti-IgG antibodies (1:5000 dilution) for 1 h. The plates were washed three additional times, and color development was initiated with 3,3′,5,5′-tetramethylbenzidine substrate (TMB; Acrobiosystems). The reaction was stopped with sulfuric acid solution. The optical density at 450 nm was measured using a Multimode Plate Reader (VICTOR Nivo; Thermo Fisher Scientific).

Quantitative real-time PCR

Cellular total RNA was isolated using TRIzol reagent (Invitrogen) following the standard protocol provided by the manufacturer. First-strand complementary DNA (cDNA) was subsequently synthesized from the extracted RNA employing the HiScript II 1st Strand cDNA Synthesis Kit (Vazyme). For quantitative realtime PCR analysis, the resulting cDNA templates were combined with HiScript III RT SuperMix for qPCR (Vazyme) together with gene-specific primer pairs. Amplification and fluorescence detection were performed on a Bioer 9600 FQD-96A real-time PCR detection system (Bioer, Hangzhou, China). Relative expression levels were normalized to the endogenous control gene *β-actin*. All primer sequences utilized in the current investigation are provided in Supplementary Table S3.

H&E staining of tissues and serological tests

After experiments, the mice were euthanized. Major organs (lung, heart, liver, kidney, and spleen) were collected and fixed in 4% paraformaldehyde. All organs were then embedded in paraffin and sectioned at 5-μm thickness. The sections were stained with H&E for histopathological evaluation. For serological analysis, blood samples were collected, and serum was obtained by centrifugation at 825 *g* for 20 min. Serum levels of alanine transaminase (ALT), aspartate transaminase (AST), alkaline phosphatase (ALP), total bilirubin (TBIL), creatinine (CRE), urea, albumin (ALB), and uric acid (UA) were measured.

Statistical analysis

All experiments were performed with at least three independent replicates. Statistical data were graphed and analyzed using GraphPad Prism (version 8.0.2; GraphPad Software, Inc., San Diego, USA) and ImageJ. Data are expressed as the mean ± standard deviation (SD). Sample sizes for each statistical analysis are noted in the figure legends. Comparisons between multiple group comparisons were analyzed by one-way ANOVA followed by Tukey's *post-hoc* test. $P < 0.05$ was considered statistically significant.

Results

Screening of signal peptides for enhanced antigen expression in mRNA vaccines

The selection of an efficient signal peptide is crucial for optimizing antigen expression and secretion in mRNA vaccines, as it directs nascent proteins into the secretory pathway [15]. Given that the efficiency of antigen secretion into the extracellular space is a critical determinant of mRNA vaccine immunogenicity, this study focused on protein families with naturally high secretory capacity, such as complement proteins present at high levels in serum and interleukins efficiently secreted by immune cells, to evaluate the impact of different signal peptides on antigen production and release. In addition, several other commonly secreted proteins were included, namely, azurocidin, insulin, coagulation factor VII, and albumin [23,24] (Supplementary Table S4). We hypothesized that signal peptides derived from such highly secreted proteins might confer similar advantages when fused to heterologous antigens. Each corresponding expression construct was engineered accordingly, as illustrated in Figure 1A.

The synthesized mRNA was encapsulated in LNPs composed of SM102, DSPC, cholesterol (CHO-HP), and PEG-2000 [25,26]. The morphology of the formulated mRNA vaccines is shown in Figure 1B. The particle size distribution had a polydispersity index (PDI) of 0.107 and a zeta potential of 0.517 mV (Figure 1C). The mRNAs encoding RBD and Nluc, engineered with different signal peptides, were co-transfected into 293T cells together with Fluc mRNA as an internal control to normalize transfection efficiency. Translation efficiency was quantitatively assessed using a dual luciferase reporter system, and the relative antigen expression level for each sample was calculated as the Nluc/Fluc ratio and normalized to the wild-type (WT) group (set as 1). The results showed that C3, C4, IL-3, and IL-12 signal peptides increased downstream antigen expression by approximately 1.5- to 2-fold, while IL-20 increased expression by 2- to 4-fold (Figure 1D). A similar trend was observed for secreted protein levels. Subsequent ELISA experiments confirmed that C3, IL-12 and IL-20 signal peptides all significantly increased the production of intracellular and secreted antigens (Figure 1E). These results indicate that different signal peptides exhibit significant differences in their ability to induce downstream antigen expression.

In vivo imaging systems revealed that at 6, 12, and 24 h, bioluminescence intensity was higher in all experimental groups than in the WT group, with the most significant increase observed in the IL-12 signal peptide group (Figure 1F). Quantitative analysis showed that at 6 h, bioluminescence intensity was higher in the C3 and IL-12 groups than in the WT group. By 12 h, the average signal intensity across all modified groups was approximately 2-fold that of the WT group. A significant increase in signal intensity was evident in the IL-12 group at 24 h. Combined with *in vitro* experimental data, these results indicate that C3, IL-12, and IL-20 signal peptides can effectively and sustainably enhance antigen expression. Therefore, these three candidates were selected for subsequent investigations.

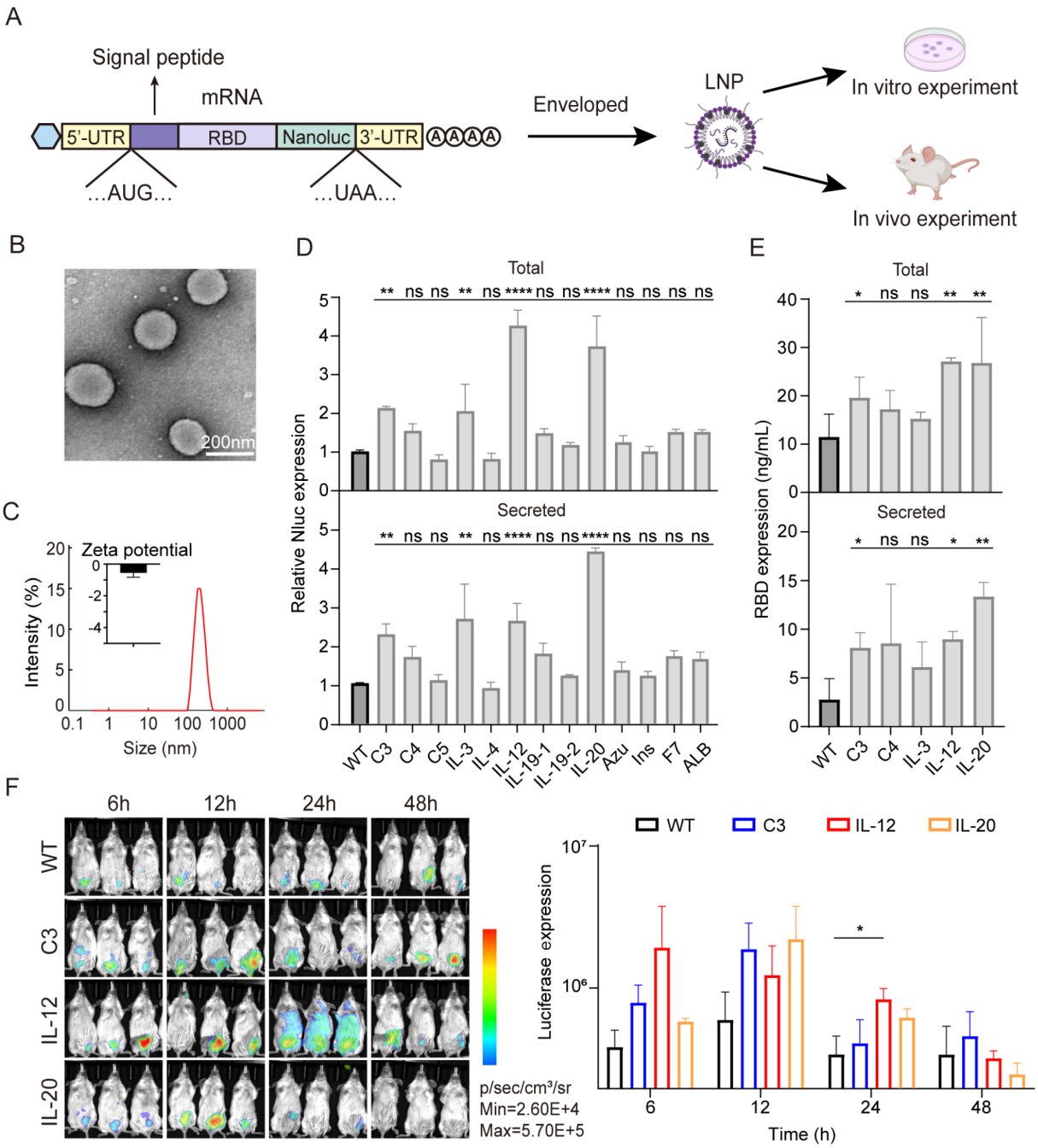


Figure 1. Screening of natural signal peptides for mediating efficient expression and secretion of downstream antigenic proteins (A) Flow chart demonstrating the mRNA vaccine preparation and experimental process. (B) Detailed visualization of the LNPs by transmission electron microscopy. (C) A representative size distribution diagram shows the range of particle sizes and the zeta potential of the LNPs, indicating their surface charge characteristics. (D) Screening of signal peptides in common secreted proteins (n = 3). (E) Selected signal peptides induced total and secreted RBD protein expression levels detected by ELISA (n = 3). (F) The distribution and expression levels of the mRNA vaccines *in vivo* were assessed following injection of the mice. Images are shown with a unified color scale. Representative images are shown (n = 4). Data are presented as the mean ± SD. *P < 0.05, **P < 0.01, ****P < 0.0001. ns, not significant.

Signal peptide replacements exhibit varying degrees of compatibility across different cell types and antigens

To investigate the cellular generality of selected signal peptides, their performance was examined across the dendritic cell line DC2.4 (an antigen-presenting cell model), the epithelial carcinoma line HeLa, and the macrophage line RAW264.7 (Figure 2A). In all three cell lines (DC2.4, HeLa, and RAW264.7), all tested signal peptide replacements enhanced total antigen expression (Figure 2B–D). However, the capacity of these signal peptides to promote antigen secretion exhibited pronounced celltype specificity. In DC2.4 cells, all three signal peptides significantly increased secretion; in HeLa cells, only the C3 signal peptide showed a robust secretory enhancement, whereas in RAW264.7 cells, a specific facilitatory effect on secretion was observed exclusively with the IL-12 signal

peptide. These findings suggest that although signal peptide replacements broadly improve translational output, their impact on the secretory pathway depends on the cell type.

Further evaluation of the antigenic generality of the selected signal peptides (C3, IL-12, and IL-20) was conducted by replacing the RBD with the respiratory syncytial virus fusion protein (RSV-F) and the Ebola virus glycoprotein (Ebola-GP) [2,27] (Supplementary Table S1). Their relative luciferase expression levels confirmed that these signal peptides successfully mediated the expression of heterologous antigens, with all three signal peptides increasing RSV-F yield by approximately 2-fold. For Ebola-GP, C3 and IL-20 increased its yield by approximately 1.6-fold (Figure 2E,F). However, their optimization profiles demonstrated clear antigen dependence and functional preferences. Furthermore, IL-20 promoted the secretion of both antigens, whereas C3 and IL-12 enhanced the secretion of Ebola-GP and RSV-F, respectively. Overall, these findings demonstrate that the selected signal peptides mediate the expression and secretion of RBDs while revealing that their compatibility is influenced by specific cellular and antigenic contexts.

Signal peptides induce ER targeting of mRNA vaccines

The classical function of signal peptides is to direct nascent proteins into the ER. To investigate the mechanism by which signal peptide

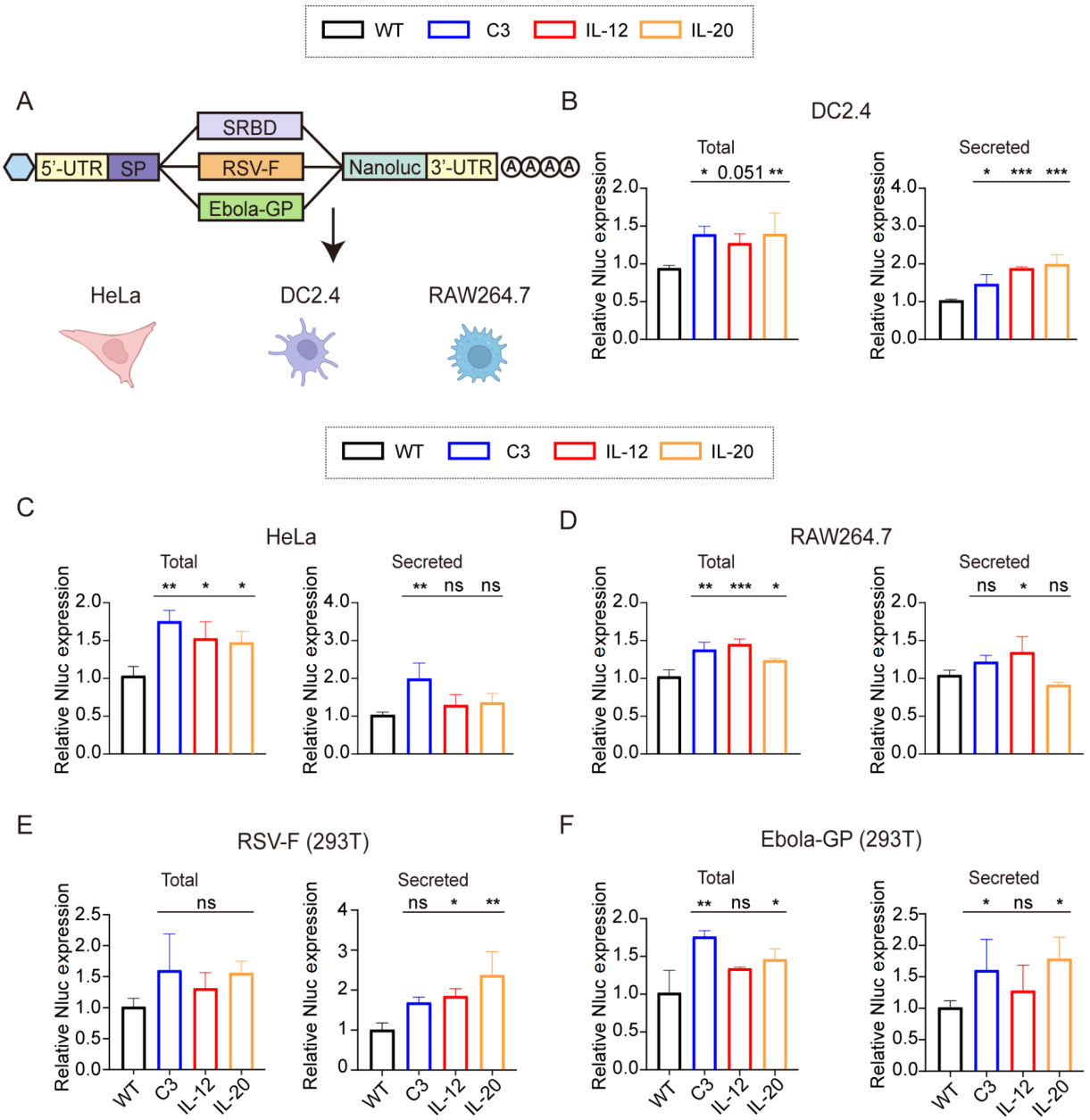


Figure 2. The enhancement of antigen expression and secretion by different signal peptides exhibits cellular and antigenic specificity (A) Schematic diagram of cellular and antigenic generality assessment. (B–D) Effects of signal peptide replacement on total and secreted antigen expression in DC2.4, HeLa, and RAW264.7 cells ($n = 3$). (E,F) Effect of signal peptide replacements on total and secreted antigen expression of RSV-F and Ebola-GP proteins in 293T cells ($n = 3$). Data are presented as the mean ± SD. $^{*}P < 0.05$, $^{**}P < 0.01$, $^{***}P < 0.001$. ns, not significant.

replacement enhances mRNA translation and secretion, fluorescence confocal microscopy was used to determine whether engineered signal peptides mediate increased mRNA targeting to the ER. The ER was visualized by transfecting 293T cells with a fusion plasmid expressing SEC61B-GFP (an established ER marker protein) [28]. After 24 h, Cy5-UTP-labeled mRNA was transfected, and its subcellular localization was examined 4 h later [29,30] (Figure 3A). Grayscale analysis revealed that mRNA-ER colocalization was increased in all experimental groups compared to the WT group (Figure 3B). Furthermore, quantitative analyses using both Pearson's correlation coefficient and Manders' coefficient indicated a significant increase in mRNA-ER co-localization in the experimental groups, with the most significant enhancement observed in the IL-12 signal peptide group, confirming that the selected signal peptides promote mRNA targeting to the ER (Figure 3C).

Further investigation was conducted to determine whether signal peptide replacement affects mRNA stability. The mRNA vaccines, each containing a different signal peptide, were transfected into 293T cells. The culture medium was replaced 2 h after transfection, and this time point was designated 0 h. Cells were then harvested at 0, 1, 2, and 4 h relative to this time point. The remaining mRNA levels were quantified using RT-qPCR, and the halflives for each group were calculated. The results showed that the halflives for WT, C3, IL-12, and IL-20 were 1.735, 1.627, 1.803, and 1.789 h, respectively (Supplementary Figure S2). These findings indicate that signal peptide replacement has minimal impact on mRNA stability, and the enhanced antigen expression observed is primarily attributable to improved translational efficiency rather than differences in mRNA stability.

Signal peptide-replaced mRNA vaccines induce stronger immune responses

To evaluate the efficacy of the signal peptide-replaced mRNA vaccine, the modified mRNA vaccine's capacity to activate SARS-CoV-2-specific B cell responses was evaluated. Following the timeline shown in Figure 4A, BALB/c mice were immunized intramuscularly with 5 μg of the respective mRNA-LNP formulations on days 0 and 21. Serum analyses conducted on day 14 (post-prime) and day 35 (post-boost) revealed a consistent and significant enhancement in antigen-specific immunity. The signal peptide-replaced mRNA vaccine induced higher levels of SARS-CoV-2-specific IgG antibodies (Figure 4B). The sustained rise in IgG levels indicates a stronger stimulus for B-cell activation and plasma cell differentiation.

Although elevated serum IgG levels are a key indicator of vaccine efficacy, the quality and durability of humoral immune protection depend largely on the establishment and composition of antigen-specific memory B cell compartments. A deeper phenotypic analysis of B cells on day 35 revealed functional divergence among the signal peptides. Only the IL-12 signal peptide significantly increased the frequencies of both RBD-specific $B220^{+}/CD21/35^{+}$ and $B220^{-}/CD21/35^{+}$ cells in the spleen (Figure 4C,D). This phenomenon reveals a key insight: the IL-12 signal peptide possesses an additional, distinct immunomodulatory property capable of specifically shaping the cellular architecture of the humoral immune response [31].

Moreover, Th cells support the B-cell response, while Tc cells can

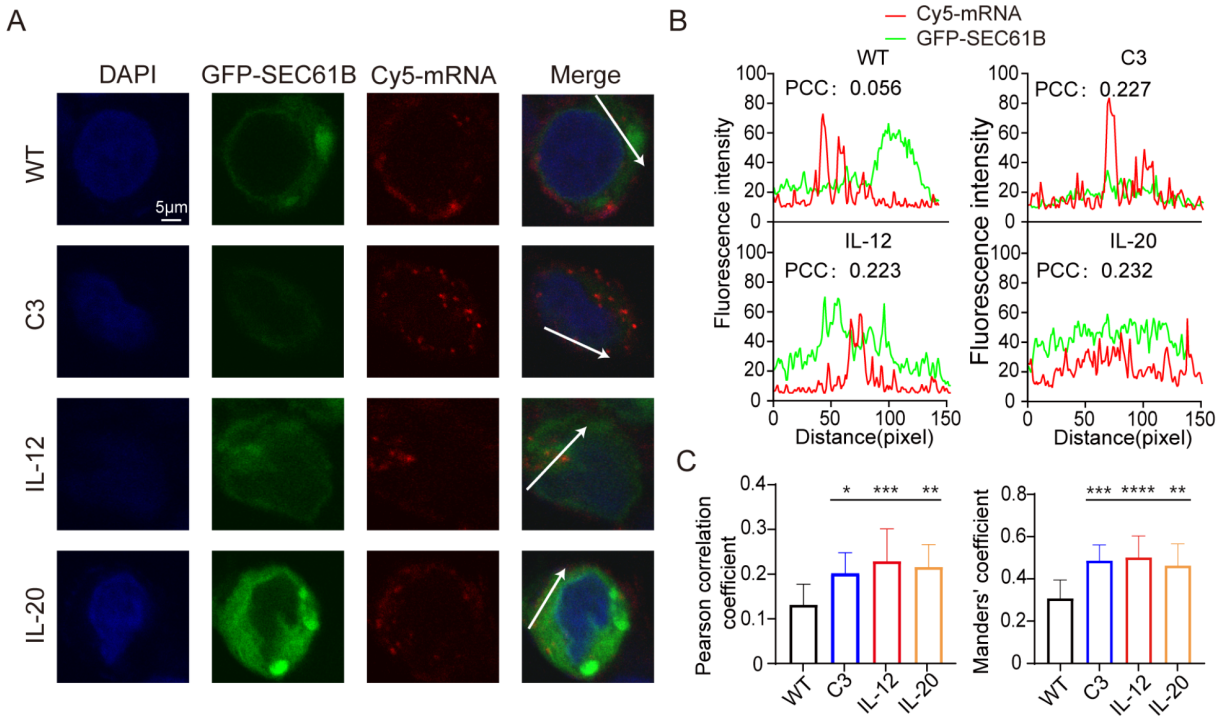


Figure 3. Signal peptide replacements of mRNA vaccines induce enhanced mRNA-ER co-localization (A) Laser scanning confocal microscopy of Cy5-mRNA (red) in 293T cells. SEC61B-GFP visualizes the ER (green). Representative images are shown (scale bar = 5 μm). (B) The graph displays the fluorescence intensity of Cy5-mRNA (red) and SEC61B-GFP (green) measured along the linear region of interest (white line) defined in the merged image of (A). (C) Pearson's correlation coefficient and Manders' overlap coefficient were calculated for each group. Data are presented as the mean ± SD from 20 individual cells per group quantified from a single representative experiment. $^{*}P < 0.05$, $^{**}P < 0.01$, $^{***}P < 0.001$, $^{****}P < 0.0001$.

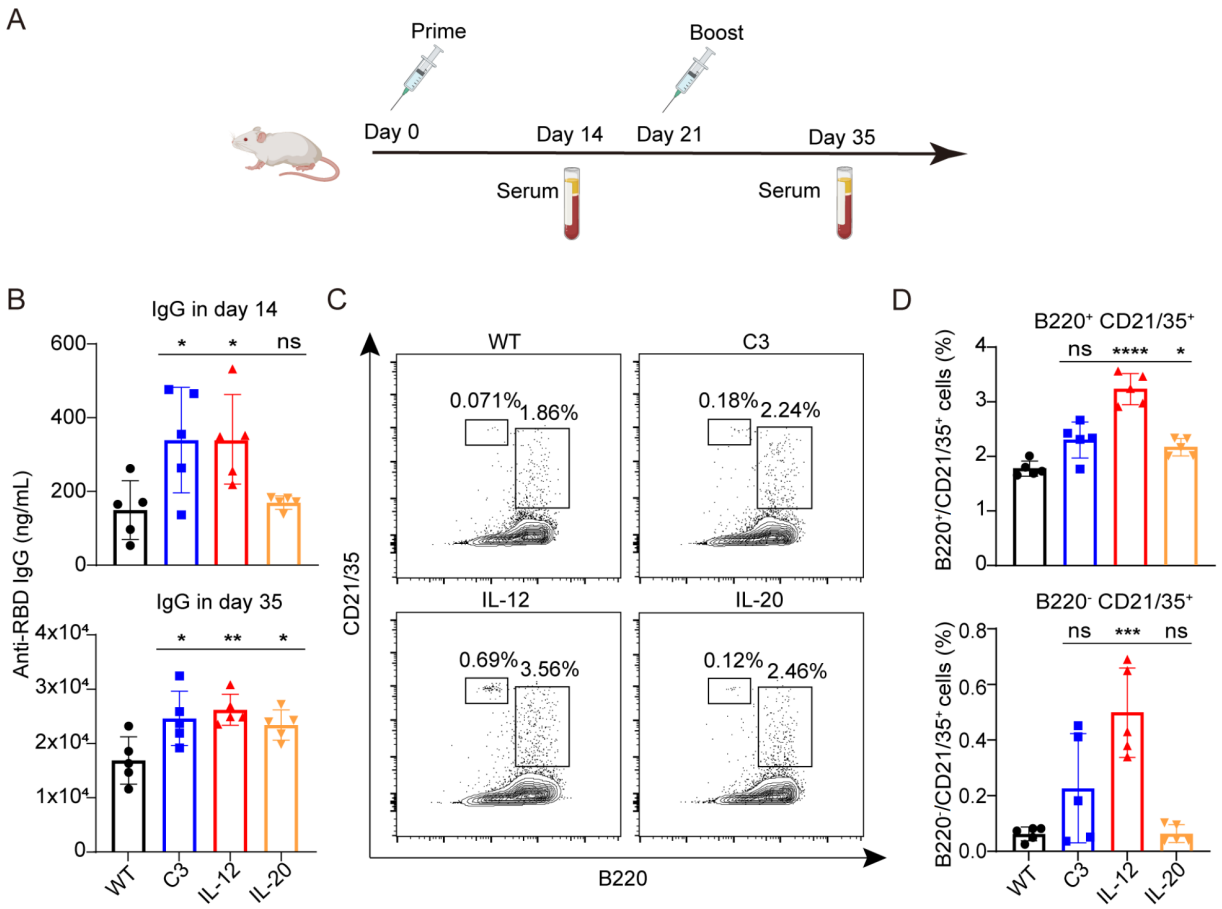


Figure 4. Signal peptide replacements lead to enhanced B cell responses induced by mRNA vaccines (A) The timeline of the therapeutic procedures was diagrammed. (B) The RBD IgG level in serum at days 14 and 35 following administration of RBD mRNA vaccines with different signal peptides detected by ELISA (n = 5). (C) Flow cytometric analysis of $B220^+$ and $CD21/35^+$ B cells induced by signal peptide replacements of mRNA vaccines. (D) Quantification of $B220^+/CD21/35^+$ cells and $B220^-/CD21/35^+$ cells in splenocytes on day 35 after vaccination (n = 5). Data are presented as the mean ± SD. $^*P < 0.05$, $^{**}P < 0.01$, $^{***}P < 0.001$, $^{****}P < 0.0001$. ns, not significant.

directly kill virus-infected cells. We detected IFN-γ- and IL-4-secreting memory Th/Tc cells within $CD4^+/CD8^+$ cells (Figure 5A). Subsequently, we assessed the ability of splenocytes to secrete cytokines using an ELISA (Figure 5B). The results indicated that, with the exception of IL-4, signal peptide replacement led to an increased trend in the secretion of IFN-γ and TNF-α. Furthermore, analysis of the proportions of Tem and Tcm cells and their ratios within $CD4^+$ and $CD8^+$ T cells revealed that the IL-12 signal peptide facilitated the differentiation of memory T cells toward an effector phenotype, resulting in a significantly enhanced Tem/Tcm ratio (Figure 5C,D). These findings suggest that the immunostimulatory effects elicited by different signal peptides may involve distinct underlying mechanisms. The mechanism by which the IL-12 signal peptide modulates the Tem/Tcm ratio warrants further investigation.

Safety evaluation and bioeffects of mRNA vaccines with different signal sequences

Comprehensive safety evaluation constitutes an essential aspect of mRNA vaccine development. Histopathological examination (H&E staining) of major organs (heart, liver, spleen, lungs, and kidneys) following treatment revealed no evident signs of inflammatory cell infiltration, necrosis, fibrosis, or architectural distortion in any of the experimental groups (Figure 6A), indicating that the engineered signal peptides did not induce visible pathological damage to target or immune organs.

Concurrently, quantitative analysis was performed on blood biochemical markers reflecting hepatic, renal, and metabolic function. There were no statistically significant differences in kidney function markers (CRE and UREA), liver function markers (TBIL, ALT, AST, ALP, and ALB), or purine metabolism marker (UA) across all groups, with all values falling within the normal physiological range (Figure 6B). These data further confirm that the modified mRNA vaccines did not induce significant hepatorenal dysfunction or systemic metabolic disturbances.

Discussion

In this study, we screened a panel of signal peptides derived from common secretory proteins. Three natural signal peptides (C3, IL-12, and IL-20) were identified that enhance antigen expression and secretion. These signal peptides promote the targeting of mRNA to the ER at the subcellular level. Importantly, these signal peptides substantially enhanced immunogenicity *in vivo*, providing a broadly applicable strategy for using signal peptides to boost the efficacy of mRNA vaccines.

Our study shows that although C3, IL-12, and IL-20 signal

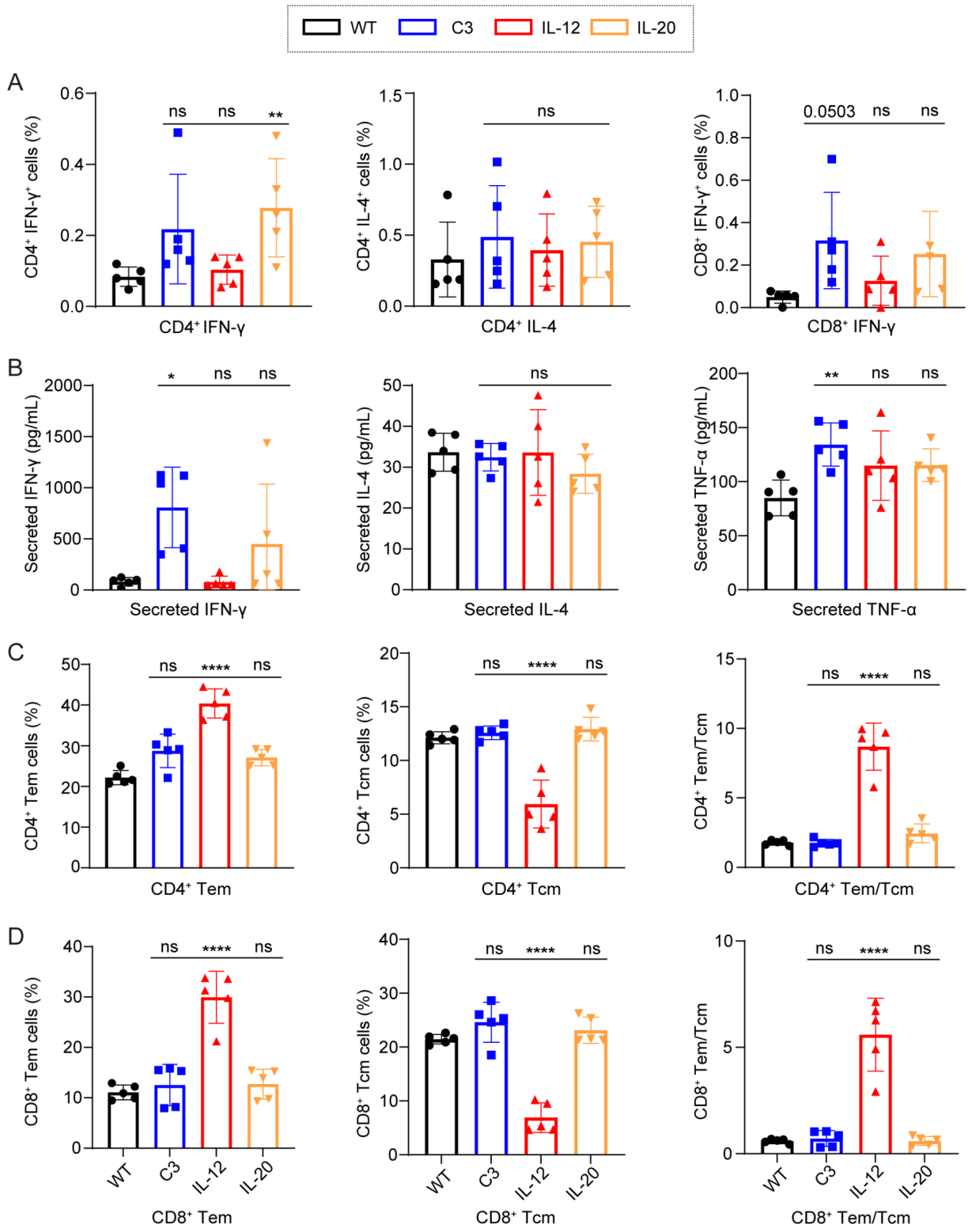


Figure 5. Different signal peptide replacements in mRNA vaccines elicit differential T cell responses (A) Flow cytometric analysis of IFN-γ⁺/IL-4⁺ CD4⁺ T cells and IFN-γ⁺CD8⁺ T cells in splenocytes on day 35 after vaccination ($n = 5$). (B) Detection of secreted IL-4, IFN-γ, and TNF-α in supernatants from splenocytes by ELISA ($n = 5$). (C) Flow cytometry was used to analyze the Tem (CD44⁺CD62L⁻) and Tcm (CD44⁺CD62L⁺) subsets within CD4⁺ T cells in splenocytes on day 35 after vaccination ($n = 5$). (D) Flow cytometry was used to analyze the Tem (CD44⁺CD62L⁻) and Tcm (CD44⁺CD62L⁺) subsets within CD8⁺ T cells in splenocytes on day 35 after vaccination ($n = 5$). Data are presented as the mean ± SD. *$P < 0.05$, **$P < 0.01$, ****$P < 0.0001$. ns, not significant.

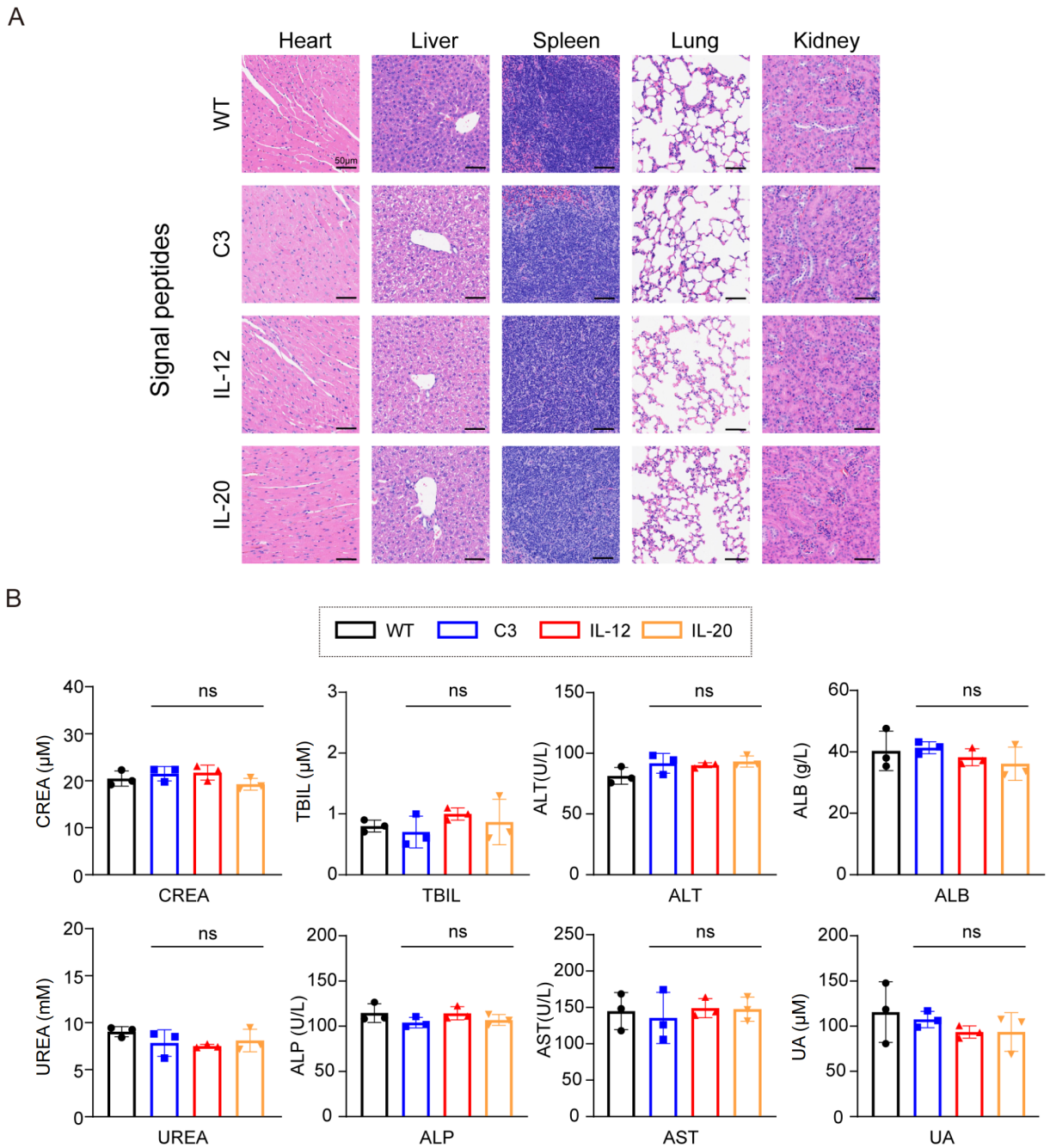


Figure 6. Safety evaluation of mRNA vaccines with signal sequence modifications (A) Histopathological analysis (H&E staining) of major organs (heart, liver, spleen, lung, and kidney) from BALB/c mice on day 35 post-immunization (scale bar = 50 μm; *n* = 3). (B) Blood biochemical criterion assessing creatinine (CREA), urea (UREA), total bilirubin (TBIL), alanine aminotransferase (ALT), aspartate aminotransferase (AST), alkaline phosphatase (ALP), albumin (ALB) and uric acid (UA) in mice intramuscularly injected with 5 μg mRNA-LNP vaccines (*n* = 3). Data are presented as the mean ± SD. ns, not significant.

peptides can promote total antigen expression across multiple cell lines (*e.g.*, 293T, DC2.4, HeLa, and RAW264.7), their enhancing effects on antigen secretion exhibit clear celltype specificity. For instance, IL-12 significantly enhances secretion in DC2.4 cells but has a weaker effect in HeLa and RAW264.7 cells. These results suggest that the function of different signal peptides may depend not only on their intrinsic sequences but also on cell-type-specific secretory machinery, ER stress thresholds or protein folding capacity. One possible explanation for this cell line-dependent effect lies in differential mRNA-ER co-localization efficiency. Our confocal imaging data (Figure 3) demonstrate that the selected signal peptides promote varying degrees of ER targeting in 293T cells; the extent of this co-localization may differ across cell types, potentially due to variations in the expression or activity of key components of the translocation machinery, such as the signal recognition particle (SRP), its receptors, or translocon-associated

proteins [32–34]. Future studies directly comparing ER localization of mRNA across different cell lines will help establish whether cell type-specific secretion patterns correlate with differences in mRNA-ER proximity.

Another notable observation is that different signal peptides differentially influence secretion efficiency despite exhibiting comparable total expression levels. For example, in 293T cells, the total antigen expression levels of IL-12 and IL-20 were comparable (Figure 1D,E), yet their secretion efficiencies differed markedly, with IL-20 exhibiting a higher proportion of secretion. Previous studies have shown that the net positive charge and hydrophobicity of signal peptides are critical determinants of SRP recognition and translocation efficiency, with modifications to the hydrophobic core of the signal peptide capable of markedly altering secretion levels [35–37]. The observed dissociation between total expression and secretion levels highlights that when optimizing signal peptides for vaccine applications, one should consider not only the protein source but also physicochemical parameters such as hydrophobicity, net charge, and helical propensity to achieve higher secretion efficiency.

Moreover, it is worth noting that our screening strategy focused primarily on signal peptides derived from constitutively secreted or immune-related proteins (such as complement factors, interleukins, and abundant serum proteins), which may have introduced a degree of bias toward certain secretory pathways. Consequently, the results may partly reflect the inherent characteristics of the screened protein families. Expanding future screening efforts to include signal peptides from a broader range of protein families and tissue sources (*e.g.*, those derived from tPA, IL-2, and IgE) would facilitate the exploration of a full sequence-function landscape. Future studies could employ proteomic profiling to compare the expression of ER chaperones, secretory vesicle components, and transport proteins across different cell lines, thereby helping to elucidate the regulatory networks underlying this specificity [38,39].

Flow cytometry analysis uncovered the complexity and functional divergence of immune responses elicited by different signal peptides. Although all selected signal peptides increased antigen yield *in vitro*, their induced cytokine profiles *in vivo* (*e.g.*, IFN-γ, TNF-α, and IL-4) did not follow a similar trend, implying that other cellular factors—such as the immune microenvironment, the activation status of antigen-presenting cells, and cytokine networks—may play important regulatory roles. Notably, the IL-12 signal peptide displayed distinct immunomodulatory properties: it not only significantly enhanced IgG output but also specifically expanded the $B220^{-}/CD21/35^{+}$ B-cell subset and drove $CD4^{+}$ and $CD8^{+}$ T-cell differentiation toward an effector-memory (Tem) phenotype, thereby markedly increasing the Tem/Tcm ratio. Although the current panel of markers provides useful characterization, future studies incorporating additional markers could dissect functional subsets in greater detail and further elucidate the immunomodulatory mechanisms underlying signal peptide-mediated effects. In conclusion, these observations strongly suggest that the IL-12 signal peptide may trigger responses independent of classical ER-targeting functions. Further studies using chimeric/truncated peptides, receptor-blocking antibodies, or single-cell transcriptomics could help identify the key functional domains and downstream signaling pathways responsible for this immunomodulatory activity.

Fluorescence confocal microscopy has confirmed that certain signal peptides promote mRNA-ER colocalization, providing important spatial evidence for the observed functional enhancement. To establish more precise quantitative and mechanistic relationships, future studies should prioritize research in the following key areas. First, it is essential to determine both the amount and translational activity of mRNAs localized near the ER, which can be achieved through ER membrane isolation combined with quantitative PCR or single-molecule fluorescence *in situ* hybridization (smFISH) [40]. Furthermore, ribosome profiling or global translation assays can assess whether the observed colocalization indeed leads to increased ribosome loading on target transcripts [41]. Finally, the proportion and kinetics of nascent antigen entering the secretory pathway require rigorous quantification. Establishing a quantitative model that links ER-targeting efficiency, translation rate, secretory efficiency, and immunogenicity will provide a powerful framework for the rational design and predictive optimization of mRNA vaccines [38].

In summary, this study not only validated that signal peptide replacement is an effective strategy for enhancing mRNA vaccine efficacy but also revealed the complexity of signal peptide functions, encompassing cell-type specificity, immune-modulatory diversity, and mechanistic depth. Future research should shift from global enhancement to precision regulation, integrating computational design, high-throughput screening and multi-omics analysis to develop a new generation of signal peptides that combine efficient targeting with immunomodulatory properties, thereby advancing mRNA vaccine platforms toward safer and more effective applications.

Supplementary Data

Supplementary data are available at *Acta Biochimica et Biophysica Sinica* online.

Data Availability

The data that support the findings of this study are available from the corresponding author upon reasonable request.

Author Contributions

Z.G. and L.R. conceptualized the study, performed the investigation and formal analysis, and drafted the original manuscript. J.F. and N.B. contributed to the methodology and validation. H.H. and Z.W. participated in partial investigation. H.D. provided critical revision of the manuscript. Y.J. polished the final version of the manuscript and figures. All authors have read and approved the final manuscript.

Funding

This work was supported by the grants from the National Key Research and Development Program of China (No. 2023YFC2604300), the National Natural Science Foundation of China (No. 92581117), the “Pioneer” and “Leading Goose” R&D Program of Zhejiang (No. 2025C01138), the Natural Science Foundation of Zhejiang Province (No. LZ25C050001), the Fundamental Research Funds for the Central Universities (No. K20220228), and the Starry Night Science Fund at Shanghai Institute for Advanced Study of Zhejiang University (No. SN-ZJU-SIAS-009).

Conflict of Interest

The authors declare they have no conflict of interest.

References

1. Pardi N, Hogan MJ, Porter FW, Weissman D. mRNA vaccines—a new era in vaccinology. *Nat Rev Drug Discov* 2018, 17: 261–279
2. Chaudhary N, Weissman D, Whitehead KA. mRNA vaccines for infectious diseases: principles, delivery and clinical translation. *Nat Rev Drug Discov* 2021, 20: 817–838
3. Zong Y, Lin Y, Wei T, Cheng Q. Lipid nanoparticle (LNP) enables mRNA delivery for cancer therapy. *Adv Mater* 2023, 35: 2303261
4. Fu J, Dong H, Wu J, Jin Y. Emerging progress of RNA-based antitumor therapeutics. *Int J Biol Sci* 2023, 19: 3159–3183
5. Navid Talemi M, Ramezani Farani M, Alipour Eskandani N, Mirzaee D, Alipourfard I, Huh YS. Programmable lipid nanoparticles for RNA therapeutics: design principles and clinical translation. *Mater Today Bio* 2026, 37: 102774
6. Fu J, Wu S, Bao N, Wu L, Qu H, Wang Z, Dong H, ***et al.*** A universal strategy of anti-tumor mRNA vaccine by harnessing "off-the-shelf" immunity. *Adv Sci* 2025, 12: 2401287
7. Shen J, Wang J, Hao Q, Ji W, Peng H, Wu Y, Zhao R, ***et al.*** Transformable nanotheranostics capable of sensoring nucleic acid drugs' spatiotemporal behaviors. *Adv Funct Mater* 2023, 33: 2209749
8. Cheng LC, Zheng D, Zhang Q, Guvenek A, Cheng H, Tian B. Alternative 3′ UTRs play a widespread role in translation-independent mRNA association with the endoplasmic reticulum. *Cell Rep* 2021, 36: 109407
9. Li X, Li Z, Zhou Y, Gong S, Chen Z, Li J, Guo M, ***et al.*** RNA G-quadruplexes promote codon repeat-associated ribosomal frameshifting in human genes. *Nucleic Acids Res* 2026, 54: gkaf1481
10. Ren G, Gu X, Zhang L, Gong S, Song S, Chen S, Chen Z, ***et al.*** Ribosomal frameshifting at normal codon repeats recodes functional chimeric proteins in human. *Nucleic Acids Res* 2024, 52: 2463–2479
11. Fu J, Liu Y, Zhong Z, Cao B, Ran L, Guo Z, Dong H, ***et al.*** mRNA lipid-nanoparticle-mediated mitochondrial apoptosis augments adoptive T cell immunotherapy. *Cell Rep Med* 2026, 7: 102706
12. Zhang Y, Zhai S, Huang H, Qin S, Sun M, Chen Y, Lan X, ***et al.*** Efficient signal sequence of mRNA vaccines enhances the antigen expression to expand the immune protection against viral infection. *J Nanobiotechnol* 2024, 22: 295
13. Kober L, Zehe C, Bode J. Optimized signal peptides for the development of high expressing CHO cell lines. *Biotech Bioeng* 2013, 110: 1164–1173
14. Horste EL, Fansler MM, Cai T, Chen X, Mitschka S, Zhen G, Lee FCY, ***et al.*** Subcytoplasmic location of translation controls protein output. *Mol Cell* 2023, 83: 4509–4523.e11
15. Choi H, Liao YC, Yoon YJ, Grimm J, Wang N, Lavis LD, Singer RH, ***et al.*** Secretome translation shaped by lysosomes and lunapark-marked ER junctions. *Nature* 2026, 649: 227–236
16. Barlowe CK, Miller EA. Secretory protein biogenesis and traffic in the early secretory pathway. *Genetics* 2013, 193: 383–410
17. Smith MH, Ploegh HL, Weissman JS. Road to ruin: targeting proteins for degradation in the endoplasmic reticulum. *Science* 2011, 334: 1086–1090
18. Voigt F, Zhang H, Cui XA, Triebold D, Liu AX, Eglinger J, Lee ES, ***et al.*** Single-molecule quantification of translation-dependent association of mRNAs with the endoplasmic reticulum. *Cell Rep* 2017, 21: 3740–3753
19. Pryme IF. Domains of rough endoplasmic reticulum. *Mol Cell Biochem* 1989, 87: 93–103
20. Morais P, Adachi H, Yu YT. The critical contribution of pseudouridine to mRNA COVID-19 vaccines. *Front Cell Dev Biol* 2021, 9: 789427
21. Tenchov R, Bird R, Curtze AE, Zhou Q. Lipid nanoparticles—from liposomes to mRNA vaccine delivery, a landscape of research diversity and advancement. *ACS Nano* 2021, 15: 16982–17015
22. Härtlova A, Erttmann SF, Raffi FA, Schmalz AM, Resch U, Anugula S, Lienenklaus S, ***et al.*** DNA damage primes the type I interferon system via the cytosolic DNA sensor STING to promote anti-microbial innate immunity. *Immunity* 2015, 42: 332–343
23. Mayer C, Bergholdt R, Cucak H, Rolin BC, Sams A, Rosendahl A, Calvert J. Neutralizing anti-IL-20 antibody treatment significantly modulates low grade inflammation without affecting HbA1c in type 2 diabetic db/db mice. *PLoS One* 2015, 10: e0131306
24. Volk HD, Asadullah K, Gallagher G, Sabat R, Grütz G. IL-10 and its homologs: important immune mediators and emerging immunotherapeutic agents. *Trends Immunol* 2001, 22: 414–417
25. Kiaie SH, Majidi Zolbanin N, Ahmadi A, Bagherifar R, Valizadeh H, Kashanchi F, Jafari R. Recent advances in mRNA-LNP therapeutics: immunological and pharmacological aspects. *J Nanobiotechnol* 2022, 20: 276
26. Allen TM, Cullis PR. Liposomal drug delivery systems: from concept to clinical applications. *Adv Drug Deliver Rev* 2013, 65: 36–48
27. Espeseth AS, Cejas PJ, Citron MP, Wang D, DiStefano DJ, Callahan C, Donnell GO, ***et al.*** Modified mRNA/lipid nanoparticle-based vaccines expressing respiratory syncytial virus F protein variants are immunogenic and protective in rodent models of RSV infection. *NPJ Vaccines* 2020, 5: 16
28. Görlich D, Prehn S, Hartmann E, Kalies KU, Rapoport TA. A mammalian homolog of SEC61p and SECYp is associated with ribosomes and nascent polypeptides during translocation. *Cell* 1992, 71: 489–503
29. Snapp EL, Reinhart GA, Bogert BA, Lippincott-Schwartz J, Hegde RS. The organization of engaged and quiescent translocons in the endoplasmic reticulum of mammalian cells. *J Cell Biol* 2004, 164: 997–1007
30. Rinaldi AJ, Suddala KC, Walter NG. Native purification and labeling of RNA for single molecule fluorescence studies. *Methods Mol Biol* 2015, 1240: 63–95
31. Awaya T, Hara H, Moroi M. Cytokine storms and anaphylaxis following COVID-19 mRNA-LNP vaccination: mechanisms and therapeutic approaches. *Diseases* 2024, 12: 231
32. Yamada Y, Miyamoto T, Higuchi S, Ono M, Kobara H, Asaka R, Ando H, ***et al.*** cDNA expression library screening revealed novel functional genes involved in clear cell carcinogenesis of the ovary *in vitro*. *J Obstet GynaEcol* 2021, 41: 100–105
33. Liu Y, Zhou J. The P124A mutation of SRP14 alters its migration on SDS-PAGE without impacting its function. *Acta Biochim Biophys Sin* 2024, 56: 315–322
34. Linder MI, Mizoguchi Y, Hesse S, Csaba G, Tatematsu M, Łyszkiewicz M, Ziętara N, ***et al.*** Human genetic defects in SRP19 and SRPRA cause severe congenital neutropenia with distinctive proteome changes. *Blood* 2023, 141: 645–658
35. Liaci AM, Förster F. Take me home, protein roads: structural insights into signal peptide interactions during ER translocation. *Int J Mol Sci* 2021, 22: 11871
36. Zhang L, Leng Q, Mixson AJ. Alteration in the IL-2 signal peptide affects secretion of proteins *in vitro* and *in vivo*. *J Gene Med* 2005, 7: 354–365
37. Peterson JH, Woolhead CA, Bernstein HD. Basic amino acids in a distinct subset of signal peptides promote interaction with the signal recognition particle. *J Biol Chem* 2003, 278: 46155–46162
38. Upadhyay M, Gupta S. Endoplasmic reticulum secretory pathway: potential target against SARS-CoV-2. *Virus Res* 2022, 320: 198897
39. Du S, Zhu C, Ren X, Chen X, Cui X, Guan S. Regulation of secretory pathway kinase or kinase-like proteins in human cancers. *Front Immunol* 2023, 14: 942849
40. Krawczyk PS, Mazur M, Orzeł W, Gewartowska O, Jeleń S, Antczak W, Kasztelan K, ***et al.*** Re-adenylation by TENT5A enhances efficacy of SARS-CoV-2 mRNA vaccines. *Nature* 2025, 641: 984–992
41. Schott J, Reitter S, Lindner D, Grosser J, Bruer M, Shenoy A, Geiger T, ***et al.*** Nascent Ribo-Seq measures ribosomal loading time and reveals kinetic impact on ribosome density. *Nat Meth* 2021, 18: 1068–1074